Mon. Not. R. Astron. Soc. **304,** 654–668 (1999)

Properties of hot stars in the Wolf–Rayet galaxy NGC 5253 from *ISO*-SWS spectroscopy

Paul A. Crowther,[1⋆] S. C. Beck,[2] Allan J. Willis,[1] Peter S. Conti,[3] Patrick W. Morris[4,5] and Ralph S. Sutherland[6]

[1]*Department of Physics & Astronomy, University College London, Gower Street, London WC1E 6BT*
[2]*School of Physics & Astronomy of the Raymond & Beverly Sackler Faculty of Exact Sciences, Tel Aviv University, Ramat Aviv, Israel*
[3]*JILA, University of Colorado, Boulder, CO 80309, USA*
[4]*ISO Science Operation Centre, Astrophysics Division, ESA, PO Box 50727, E-28080 Villafranca, Madrid, Spain*
[5]*SRON, Sorbonnelaan 2, CA 3584 Utrecht, the Netherlands*
[6]*Mount Stromlo and Siding Spring Observatories, Australian National University, Canberra, ACT 0200, Australia*

Accepted 1998 December 2. Received 1998 November 30; in original form 1998 September 14

ABSTRACT

ISO-SWS spectroscopy of the Wolf–Rayet galaxy NGC 5253 is presented, and analysed to provide estimates of its hot young star population. Our approach differs from previous investigations in that we are able to distinguish between the regions in which different infrared fine-structure lines form, using complementary ground-based observations. The high-excitation nebular [S IV] emission is formed in a very compact region, which we attribute to the central super-star nucleus, and lower excitation [Ne II] nebular emission originates in the galactic core. We use photoionization modelling coupled with the latest theoretical O-star flux distributions to derive effective stellar temperatures and ionization parameters of $T_{\rm eff} \geq 38$ kK, $\log Q \sim 8.25$ for the compact nucleus, with $T_{\rm eff} \sim 35$ kK, $\log Q \leq 8$ for the larger core. Results are supported by more sophisticated calculations using evolutionary synthesis models. We assess the contribution that Wolf–Rayet stars may make to highly ionized nebular lines (e.g. [O IV]).

From our Brα flux, the 2-arcsec nucleus contains the equivalent of approximately 1000 O7 V star equivalents and the starburst there is 2–3 Myr old; the 20-arcsec core contains about 2500 O7 V star equivalents, with a representative age of ~5 Myr. The Lyman ionizing flux of the nucleus is equivalent to that of the 30 Doradus region. These quantities are in good agreement with the observed mid-infrared dust luminosity of 7.8×10^8 L$_\odot$. Since this structure of hot clusters embedded in cooler emission may be common in dwarf starbursts, observing a galaxy solely with a large aperture may result in confusion. Neglecting the spatial distribution of nebular emission in NGC 5253 implies 'global' stellar temperatures (or ages) of 36 kK (4.8 Myr) and 39 kK (2.9 or 4.4 Myr) from the observed [Ne III/II] and [S IV/III] line ratios, assuming $\log Q = 8$.

Key words: stars: Wolf–Rayet – galaxies: individual: NGC 5253 – galaxies: starburst – galaxies: stellar content – infrared: galaxies.

1 INTRODUCTION

Wolf–Rayet (WR) galaxies are a subset of blue emission-line galaxies the spectra of which show the signature of large numbers of WR stars (Vacca & Conti 1992). These galaxies are among the youngest starburst galaxies and contain a large population of very massive stars with ages in the range $1–10 \times 10^6$ yr. Mid-infrared (IR) observations are well suited to the study of hot, massive stars, since this spectral region contains many fine-structure nebular lines which depend very sensitively on stellar content. Until recently, use of such diagnostics was severely hindered because of the low transparency of our atmosphere at mid-IR wavelengths. The launch of the *Infrared Space Observatory* (*ISO*) has opened up this new window, which we are exploiting through a Guest Observer programme (WRGALXS: PI A. J. Willis) with the *ISO* Short Wavelength Spectrometer (SWS).

NGC 5253 is one of the closest WR galaxies, at a distance of only 4.1 Mpc (Saha et al. 1995), and represents one of the targets of our

⋆ E-mail: pac@star.ucl.ac.uk

Guest Observer programme. NGC 5253 contains several very young super-star clusters, no older than a few million years (Walsh & Roy 1989; Beck et al. 1996). It has been the focus of many recent studies (e.g. Gorjian 1996; Calzetti et al. 1997; Turner, Beck & Hurt 1997), which have shown that the extinction is very high and patchy at ultraviolet and visual wavelengths. *ISO* observations of NGC 5253 are particularly important since the interstellar extinction at mid-IR wavelengths is low and because earlier spectral observations found evidence for a remarkably hot and young stellar population (Aitken et al. 1982; Lutz et al. 1996; Beck et al. 1996).

In Section 2 we present our new *ISO*-SWS spectroscopy of NGC 5253 together with complementary ground-based observations, which are interpreted in Section 3. Our technique for photoionization modelling, based largely on CLOUDY (Ferland 1996), is discussed in Section 4, including assumed elemental abundances and theoretical flux distributions for O stars. In Section 5 we discuss the results of our photoionization modelling. The influence from WN- and WC-type Wolf–Rayet stars is considered in Section 6, while results obtained using evolutionary synthesis models are presented in Section 7. Our present results are compared with those from the literature in Section 8, and our conclusions are reached in Section 9.

2 OBSERVATIONS AND REDUCTION

Our new infrared data on NGC 5253 were obtained as part of a Guest Observer programme with the Short Wavelength Spectrograph (SWS: de Graauw et al. 1996) onboard the ESA *Infrared Space Observatory* (Kessler et al. 1996) in revolution 418, 1997 January 7.

The SWS AOT6 observing mode was used to achieve full grating resolution, $\lambda/\Delta\lambda \sim 1300-2500$, and the continuous wavelength coverage was 2.99–27.65 μm. Data of detector 'bands' 1 and 2 respectively cover wavelengths of 2.99–4.08 μm using 12 In:Sb detectors and 4.00–12.05 μm with 12 Si:Ga detectors, employing entrance slits that give an effective aperture area of 14×20 arcsec^2 on the sky. Band 3 data cover 12.0–27.65 μm using 12 Si:As detectors, with sky coverage of 14×27 arcsec^2. The total integration time was set to 9140 s to allow one complete scan over the wavelengths selected within each 'AOT band', defined by the permissible combinations of detector band, aperture and spectral order (cf. de Graauw et al. 1996). The observation time includes dark current measurements, and a monitor of photometric drift for the detectors of bands 2–3. A drift measurement is not normally made for the relatively stable In:Sb detectors.

The SWS data were processed through the main stages of raw signal conversion (bits to μV s^{-1}), glitch recognition, wavelength calibration and dark current subtraction by following the standard chain of pipeline software and calibration tables complying with version 6.0 or later. Final photometric calibrations performed in the SWS Interactive Analysis environment rely on relative spectral response functions and absolute photometric response factors that were conditional for further pipeline development. These are generally consistent with calibrations found in pipeline version 7.0. Prior to co-addition of the output of each detector, data were statistically filtered using the results of glitch recognition algorithms, rejecting data points with corresponding signal ramps that were found to have more than two departures from linearity after AC correction. Detector 27 was judged to behave photometrically unstably in this observation, and all output from it was rejected. Remaining detector output was rectified to the mean flux density within each resolution elements, 3σ points were excluded, and the data were finally re-binned to a spectral resolution that is somewhat higher than instrumental.

General aspects of the wavelength and photometric calibrations as of revolution ~100 (after initial verification of instrument performance) are described, respectively, by Valentijn et al. (1996) and Schaeidt et al. (1996). More contemporary performance details are in preparation for the *ISO* Post Mission Archive by the SWS instrument team.

2.1 Aperture orientation

The input coordinates coinciding with aperture centre were $\alpha = 13^{\rm h}39^{\rm m}55\overset{\rm s}{.}7$, $\delta = -31°38'29\overset{''}{.}0$ (J2000.0). Spacecraft pointing uncertainties are alleged to have been around 2 arcsec at the time of this pointing, following recalibration of the star-tracker CCD some 50 revolutions prior. Pointing reconstruction software in pipeline version 7.0, accounting also for later changes in solar ephemerides updating procedures, indicates offsets, both along the dispersed (corresponding to the spacecraft *Z*-axis) and orthogonal to the dispersed (*Y*-axis) directions of SWS, to be within the quoted uncertainty. The centre of our apertures is ~2 arcsec from the ultraviolet source UV3 of Kobulnicky et al. (1997), but is sufficiently large to include the strong nebular Hα- and Brα-emitting regions of NGC 5253, ≈5 arcsec from the centre of our aperture (see Kobulnicky et al. 1997; Davies, Sugai & Ward 1998). The two SWS aperture projections are overlaid on a *Hubble Space Telescope* (*HST*) WFPC2 Hα image of NGC 5253 from Calzetti et al. (1997), together with a 2-cm VLA contour map from Beck et al. (1996) in Fig. 1.

It is important to note that photometric responses are not flat over the spatial extent of the area covered by each detector block. This is most important in the direction orthogonal to the dispersion axis (along the spacecraft *Y*-axis: see Fig. 1), where an offset of 5 arcsec from the position of peak responsivity results in a loss of 20–25 per

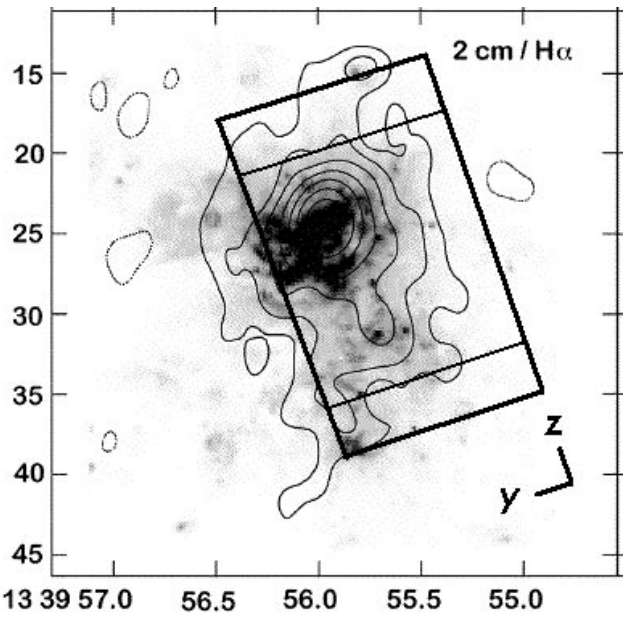

Figure 1. *ISO*-SWS apertures superimposed on the Calzetti et al. (1997) *HST*-WFPC2 Hα image of NGC 5253, together with the 2-cm VLA radio continuum contour map from Beck et al. (1996). The *ISO* aperture is 14×20 arcsec^2 for $\lambda \leq 12$ μm, and 14×27 arcsec^2 at longer wavelengths. The spacecraft *Y*- and *Z*-axes, indicated here, are discussed in the text. Declination ($-31°38'$) and right ascension ($13^{\rm h}39^{\rm m}$) are in J2000.0 coordinates.

cent flux of combined detector output from a point source. The loss within 2 arcsec of the aperture centre is less than 5 per cent for bands 2–3, which exhibit similar beam profiles. This is shown in rough form in Schaeidt et al. (1996), but detailed profiles to the aperture edge and beyond are in analysis at this time. For band 1, the loss is negligible within ∼2.5 arcsec of the aperture centre, but a sharper gradient in responsivity beyond this again results in a loss of 20–25 per cent at ∼5 arcsec away. If 30 per cent of Brα line emission does originate from the central nucleus of NGC 5253 (cf. Davies et al. 1998), then the offset along the minor axis of the aperture may mean that the energy measured in the line is underestimated by ∼10 per cent. For more extended line emission (see below), a loss estimate is more difficult to obtain without a surface brightness distribution and knowledge of the photometric responses to the aperture edges and beyond. Overall, photometric uncertainties are estimated to be ∼5 per cent in band 1, 10–15 per cent in band 2 and 15–25 per cent in band 3. No large discrepancies between levels of adjoining AOT bands were noticed.

2.2 Infrared nebular emission-line fluxes

We present the full SWS spectrum of NGC 5253 in Fig. 2. Several sharp nebular emission lines are apparent, superimposed on a rising 'continuum' flux distribution attributed to dust emission (see Section 3.2). The most pronounced nebular lines arise from ground-state fine-structure lines of [S IV]10.51 μm, [Ne III]15.55 μm and [S III]18.71 μm; weaker nebular emissions are also seen in [Ne II]12.81 μm and [Ar III]8.99 μm. We have used the emission-line fitting routine ELF in DIPSO (Howarth et al. 1995) to measure line fluxes using an eye-estimated local continuum flux; these are presented in Table 1. Since the *ISO* aperture is offset from the central nucleus along the minor axis, we have included a 10–15 per cent correction for light loss. From the table, there are clearly additional uncertainties – the measured [S IV] flux from the small-aperture ground-based observation is *greater* than that from the large-aperture *ISO* data set.

Individual nebular line profiles are shown in Fig. 3, although these are unresolved at the SWS AOT6 resolving power. Emission lines are redshifted by $\Delta v \sim +200$ km s^{-1}, in reasonable agreement with optical measurements of the galactic recession velocity (+416 km s^{-1} from de Vaucouleurs et al. 1993). The observed Δv was used to search for weaker emission lines, allowing us to confirm the presence of Brα 4.051 μm and (possibly) Pfα 7.458 μm (see Fig. 3). We include the spectral region around [Ar II]6.99 μm in our band 2C SWS data set, although the positive identification and measured flux of this feature are uncertain, owing to its location at the edge of the 2B and 2C bands and low Δv.

Table 1. Nebular emission lines observed in our *ISO*-SWS (AOT6) spectrum of NGC 5253, and ground-based measurements. Our *ISO* fluxes are after correction for the variable profile across the beam in the spacecraft *Y*-axis (see Section 2.1).

Ion	λ_{lab} μm	Obs. Flux 10^{-16}W m^{-2}	Aperture arcsec	Source
Br–γ	2.16	1.5	10 × 20	Kawara et al. (1989)
	2.16	1.0	4	Davies et al. (1998)
	2.16	2.9	30	Davies et al. (1998)
Br-α	4.05	5.1	14 × 20	*ISO*-SWS
	4.05	7.0	10 × 20	Kawara et al. (1989)
Ar II	6.99	<4.0	14 × 20	*ISO*-SWS (band 2C)
Pf-α	7.46	≤1.0	14 × 20	*ISO*-SWS
Ar III	8.99	5.6	14 × 20	*ISO*-SWS
	8.99	3.6	1.6	Beck et al. (1996)
S IV	10.51	32.4	14 × 20	*ISO*-SWS
	10.51	39.0	1.6	Beck et al. (1996)
Ne II	12.81	11.5	14 × 27	*ISO*-SWS
	12.81	≤1.0	1.6	Beck et al. (1996)
Ne III	15.55	46.2	14 × 27	*ISO*-SWS
S III	18.71	23.0	14 × 27	*ISO*-SWS
S III	33.46	35.7	20 × 33	Genzel et al. (1998)
Si II	34.81	19.5	20 × 33	Genzel et al. (1998)

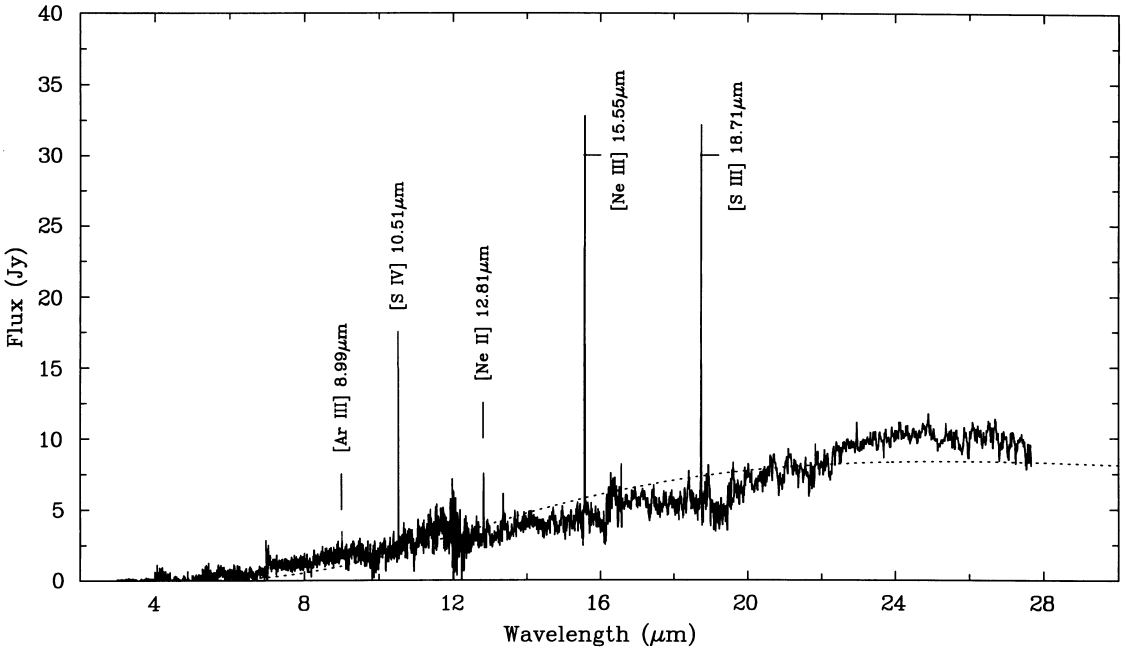

Figure 2. Flux-calibrated (in jansky) spectrum of NGC 5253 obtained with *ISO*-SWS, including a blackbody fit (dotted line) to the observed dust continuum. The broad feature between 22 and 27 μm appears to be due to solid-state silicate emission, representing the first such detection in a starburst galaxy.

We have also collected IR flux measurements for NGC 5253 from the literature, which are also included in Table 1. The hydrogen Brackett line data are taken from Kawara, Nishida & Phillips (1989) and Davies et al. (1998), and the metal lines from Beck et al. (1996). In general the *ISO*-SWS and ground-based results agree reasonably well, except for the [Ne II]12.81-μm line (see Section 3). Genzel et al. (1998) have recently presented additional [S III] and [Si II] mid-IR line flux ratios obtained with band 4 of *ISO*-SWS, obtained at a location ≈2.4 arcsec from our data set. We have converted these into absolute flux measurements using our [Ne II] measurement, although this introduces an additional uncertainty since the SWS band 4 aperture is 20×33 arcsec^2. In theory we should be able to use the observed ratio of [S III](33.5 μm/18.7 μm) of ∼1.6 to measure the (emissivity weighted) mean electron density of the [S III]-emitting region. However, these lines were obtained through apertures of different sizes, and the observed ratio is close to the low-density limit, so, applying simple nebular theory, we find $n_e < 10^{2-3}$ cm^{-3}. For comparison, Walsh & Roy (1989) obtained $n_e = 10^{2.46}$ cm^{-3} for the central $\sim 8 \times 4$ arcsec^2 of NGC 5253 from optical spectroscopy.

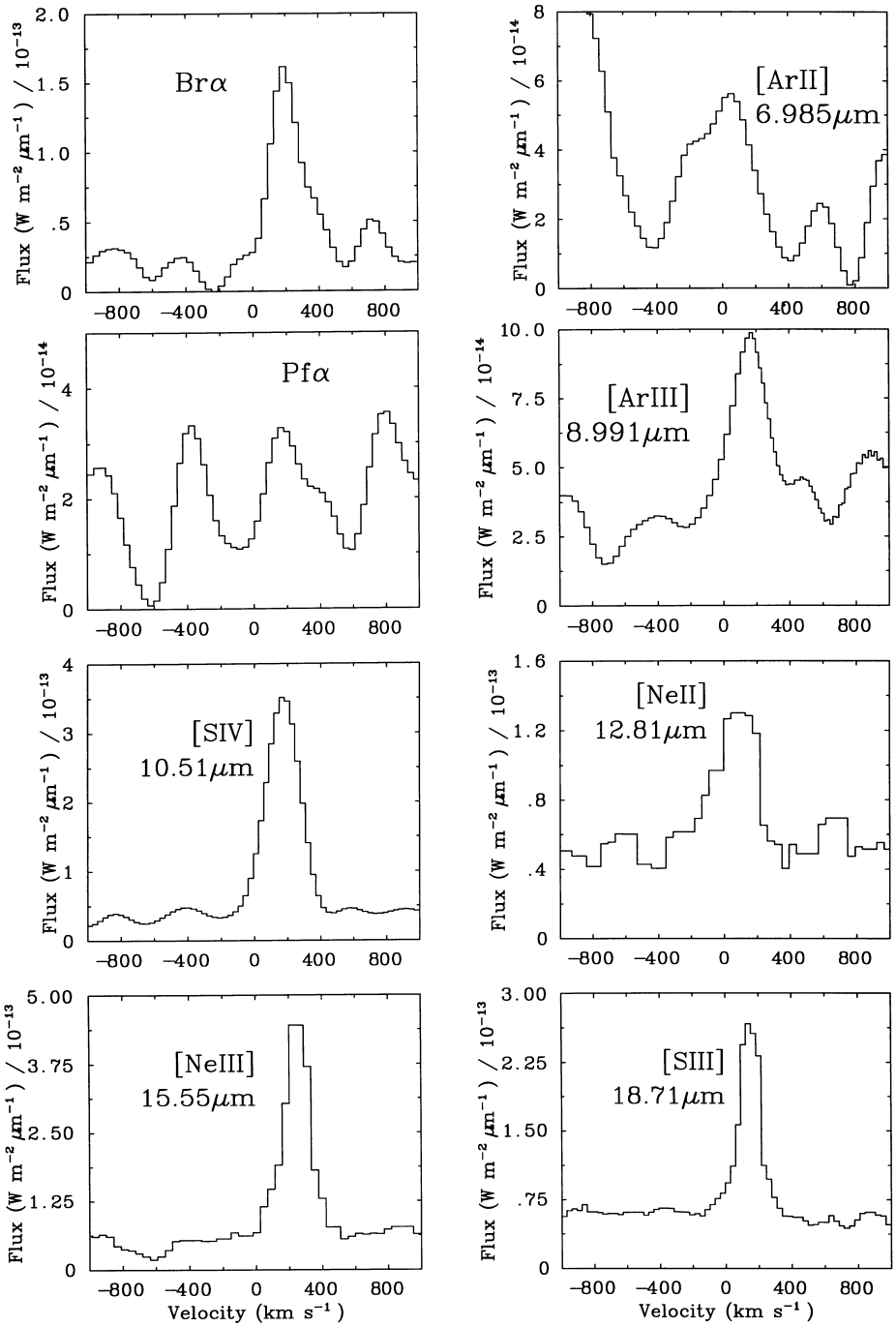

Figure 3. Principal nebular emission lines observed in the *ISO*-SWS spectrum of NGC 5253, redshifted by $\Delta v \sim +200$ km s^{-1}. The identifications of [Ar II] and Pfα are uncertain.

3 INTERPRETATION OF GROUND- AND SPACE-BASED IR OBSERVATIONS

Before we undertake a detailed analysis of our *ISO* observations, we first compare our ground- and space-based mid-IR line fluxes. We also estimate the massive stellar content of NGC 5253 from the IR dust continuum. There are potential dangers in forming line ratios when the source is a galaxy which can be expected to contain many regions of different characteristics, and especially if it is a galaxy like NGC 5253 which is known for marked spatial variations in stellar age, dust content and other features.

3.1 A hot nucleus in a cooler extended core

The IR line fluxes listed in Table 1 include both the *ISO* results and, for the [S IV], [Ne II] and [Ar III] lines, the fluxes observed from the ground with the Irshell spectrometer (Beck et al. 1996) which had a 1.6-arcsec beam; mapping showed that the [S IV] and [Ar III] detected by Irshell came from a region about 2-arcsec in diameter. Similar dimensions were found by Davies et al. (1998) for the dominant Brγ source. At the distance of NGC 5253, this corresponds to a (maximum) size of 40 pc. The most striking thing about Table 1 is the close agreement of the [S IV]10.5-μm fluxes observed with the large *ISO* beam and the 1.6-arcsec Irshell beam. This result argues that the [S IV] emission is concentrated in the inner 2–4 arcsec of the galaxy. However, we cannot assume that all the line fluxes are similarly concentrated: another feature of Table 1 is the order-of-magnitude excess of [Ne II]12.8-μm emission in the *ISO* observations compared with the ground-based ones, which is most readily explained if the [Ne II] is extended over an area comparable to the *ISO* beam so the small Irshell beam did not measure the total.

In Section 5 we shall show that [S IV] emission increases with increasing stellar temperatures and ionization parameters, with the reverse found for [Ne II]. Therefore the most natural explanation is that the [S IV] region, the central 2 arcsec mapped by Irshell, contains very hot stars at high ionization parameter, while the [Ne II] region contains cooler stars at lower Q-value. Other lines from high-ionization stages will be likely to originate in the [S IV] region and those from lower ionization in the [Ne II] region.

This is a far-reaching assumption, but the picture of NGC 5253 that has been established from high spatial resolution observations supports it. In the radio continuum, the thermal emission owing to young stars is dominated by a central source of less than 2 arcsec, which contains more than half the radio flux from the area of the *ISO* beam (Turner, Ho & Beck 1998). This radio source is extremely young, which has led it to be identified with the 'central star cluster' [S IV] source (Beck et al. 1996) and with the visually obscured cluster NGC 5253-5 of Calzetti et al. (1997), which is thought to be no more than 2.5 Myr old, resides in the centre of the starburst nucleus, and is very compact. The youth of the cluster is seen in the lack of supernova remnants and the presence of very massive and short-lived stars which are hot enough to excite strong [S IV] emission. Calzetti et al. distinguish between the starburst nucleus, which contains the central cluster, and the galactic core, which is older, produces stars at a rate about 1/10 that of the nucleus, is UV-rich, and covers an area comparable to the *ISO* beam. If the [S IV] source is associated with the starburst nucleus, the [Ne II] emission may be presumed to come from the larger core. The halo of NGC 5253 was not observed by *ISO* and is not discussed in this work.

3.2 Dust emission and the number of O stars in NGC 5253

The SWS spectrum of NGC 5253 in Fig. 2 shows that the nebular emission lines are superimposed on an underlying energy distribution which has negligible flux below 4 μm, peaks at about 10 Jy at 24 μm and then turns over to longer wavelengths. This energy distribution clearly reflects emission from relatively warm dust. The broad emission between 22.5 and 27 μm suggests possible solid-state silicate emission, a sensitive tracer of mass-loss history. This is common in O-rich environments of the Galaxy but is not known in extragalactic regions, like 30 Doradus, where the dust may be insufficiently shielded. Therefore NGC 5253 appears to be the first example of silicate emission in a starburst galaxy. Using blackbody energy distributions normalized to the SWS data at about 21 μm, we find a best fit to the observed data for a temperature of 200 $\pm$ 10 K, as shown in Fig. 2. From this, the total integrated dust emission at the Earth is 1.6×10^{-12} J s^{-1} m^{-2}. Adopting a distance of 4.1 Mpc to NGC 5253 (Saha et al. 1995), this translates into a total dust emission luminosity of 2.9×10^{35} J s^{-1}, or $L_{\rm IR} = 7.8 \times 10^8$ L$_\odot$. [For comparison, Lutz et al. (1996) report $L_{\rm IR} = 8.0 \times 10^8$ L$_\odot$ from *ISO*-SWS spectroscopy, while Stevens & Strickland (1998) derive 6.9×10^8 L$_\odot$ using *IRAS* flux measurements plus our adopted distance.]

Before we estimate the number of hot stars exciting this dust, let us recall the concept of an 'equivalent' O star (Vacca 1994). This hypothetical object was introduced so as to ease the transformation between what is measured by the Lyman continuum flux and 'the number of O stars', and provides a useful means of comparing the energetics of star formation regions in galaxies and other sources. The number of Lyman continuum photons from an O-star 'equivalent' is 10^{49} Ly photon s^{-1}, close to that of an O7 V star. Vacca (1994) calculates the correction in transforming from the number of 'equivalent' O stars to the 'number of O stars'. This depends on the initial mass function (IMF) slope, the metal abundance, and the upper mass cut-off. Roughly half of the ionizing flux comes from stars hotter and the other half from stars cooler than the O-star 'equivalent', thus the correction is typically less than a factor of 2. It should be kept in mind that one might be measuring the Lyman continuum flux and determining the number of O-star 'equivalents', and estimating the 'number of O stars', but there may only be stars of later spectral type than O7 V if the starburst is somewhat evolved. In fact, we will see this case below in the 'core' of NGC 5253.

The Lyman continuum flux of a region of hot stars is usually found from the extinction-free radio continuum, but in NGC 5253 this is partly optically thick and there is insufficient spatial resolution to determine which can be associated with the starburst nucleus and which with the core. We therefore assume that the H II region is dust-free, and optically thick to Lyman continuum radiation (Case B ionization-bounded). We adopt $n_{\rm e} = 10^{2.5}$ cm^{-3} and $T_{\rm e} = 11\,700$ K for the core (Walsh & Roy 1989) for the determination of hydrogen intensity ratios (Storey & Hummer 1995). Our extinction-corrected *ISO* Brα flux implies a total ionizing flux of 3.45×10^{52} Ly photon s^{-1}. This supports the previous determination of 4×10^{52} Ly photon s^{-1} from Hα by Martin & Kennicutt (1995), although Davies et al. (1998) recently used Brγ observations plus an aperture of 30 arcsec to derive a factor of 2 higher Lyman ionizing flux (scaled to our assumed distance). This discrepancy would be larger still (factor of 2.7) if we adopted a consistent IR extinction.

Davies et al. revealed a dominant nebular source, spatially coincident with the visual Hα emission peak, containing 30 per cent of the Brγ emission within 2 arcsec of the central nucleus. [A similar fraction was measured by Martin & Kennicutt (1995) from

Hα observations.] We therefore conclude that the ionizing flux of the nucleus, as derived from our measured Brα flux, is 1.0×10^{52} Ly photon s^{-1} – comparable to 30 Doradus (Kennicutt 1984) – and that the ionizing flux in the core is 2.5×10^{52} Ly photon s^{-1}. The total ionization is equal to 3500 equivalent O7 V stars.

Using the recent O-star calibration of Vacca, Garmany & Shull (1996), we find a luminosity of $\sim 2.5 \times 10^5$ L$_\odot$ for an O7 V star. With the typical assumption that the dust luminosity is governed by the radiation from the hot stars, our derived $L_{\rm IR}$ is equivalent to about 3100 O7 V stars. This number is in good agreement with that for the O-star 'equivalents' inferred from the Lyman continuum measures.

4 PHOTOIONIZATION CALCULATIONS

The *ISO* data on NGC 5253 include the important diagnostic lines of sulphur, argon and neon, from the ratios of which it should be possible to deduce the extreme-ultraviolet (EUV) spectrum of the input ionizing radiation, and thus the temperature of the exciting star (in a nebula excited by a single star), or the effective temperature and thus the age and mass function of an exciting cluster of stars. In the following section we will use results from a grid of model H II regions produced with the photoionization code CLOUDY (Ferland 1996). First, we describe our technique, choice of elemental abundances and O-star energy distributions, since these quantities will have a major effect on the results.

4.1 Description of the calculations

We constructed photoionization models using CLOUDY (v90.04) as described in Ferland (1996) and Ferland et al. (1998). Comparisons with other photoionization codes are provided by Ferland et al. (1995). The nebulae are represented by a sphere of uniform gas density, n, and filling factor, ϵ, with a small central cavity, which is ionized and heated solely by the UV radiation of a single central star. Nebular fluxes are predicted, given input abundances, flux distributions and physical parameters, the most important of which is the ionization parameter. This may be written as $Q = Q_{\rm H}/(4\pi R_{\rm S}^2 n)$, where $Q_{\rm H}$ is the number of ionizing photons below the H-Lyman edge at 912 Å, and $R_{\rm S}$ is the radius of the Strömgren sphere. (An alternative definition of the ionization parameter is $U = Q/c$.)

For a given energy distribution of the ionizing radiation field, any combination of parameters that keeps $Q_{\rm H} n \epsilon^2$ constant will result in an identical ionization structure of the gas (see Stasińska & Leitherer 1996). For each flux distribution we have followed Stasińska & Schaerer (1997) by computing a series of models with hydrogen density $n = 10$ cm^{-3} and $\epsilon = 1$, in which the stellar luminosity has been multiplied by a factor of 10^5, 10^4, ..., 10^{-3}. These models thus correspond to varying the ionization parameter $\log Q = 6$ to 10. This covers the range of ionization parameters expected in astrophysically relevant conditions as found by Stasińska & Leitherer (1996).

4.2 Abundance effects

The elemental abundances in the ionized gas can strongly affect the cooling of the nebula and thus the observed line ratios. NGC 5253 is seen from optical spectroscopy by Walsh & Roy (1989) to be metal-poor, with $12 + \log({\rm O/H}) = 8.17$ derived for the region centred on the major Hα (and Brγ) emission. More recently, Kobulnicky et al. (1997) have derived elemental abundances of N, O, Ne, S and Si in several regions of the core H II region from *HST* spectroscopy, and confirm a depleted metal content. They support earlier evidence for a region of enhanced nitrogen abundance, attributed to enriched material from WN stars. The abundance of sulphur is 1/4–1/2 times that of the Orion nebula (Baldwin et al. 1991). For our analysis we use abundances derived for region H II–1 by Kobulnicky et al. (1997), and 1/3 that of the Orion nebula (or approximately 1/4 solar metallicity) for elements that Kobulnicky et al. were unable to measure.

Test calculations were performed, including variation of dust grain abundances and compositions [interstellar medium (ISM), Orion]. Overall the influence of dust was not substantial, with the greatest differences obtained in high-luminosity models, such that the ionization balance and nebular temperature increase. We found that the optimum consistency between different IR diagnostics was obtained for models including ISM grains (silicate and graphite). Consequently, all models considered in this work assume this grain mixture.

4.3 Flux distributions for O-type stars

Most of the recent studies on analysis of H II regions use the Kurucz (1991) plane-parallel local thermodynamic equilibrium (LTE) model atmospheres. This is because these models include line blanketing and are available for a wide range of stellar temperatures and metallicities. However, with regard to O-type stars, Kurucz models neglect both non-LTE effects and the influence of stellar winds, with important consequences for the EUV flux distribution from such stars (e.g. Sellmaier et al. 1996; Schaerer & de Koter 1997).

We have therefore used the grid of theoretical stellar flux distributions from Schaerer & de Koter (1997). In contrast with the Kurucz (1991) O-star flux distributions, those of Schaerer & de Koter (1997) (i) differ greatly below the He II λ228 edge, and (ii) show little metallicity dependence in the important λλ228–912 region. Indeed, the Kurucz (1991) and Schaerer & de Koter (1997) flux distributions show only minor differences at low metallicities in this region. Stasińska & Schaerer (1997) have demonstrated the improved agreement between theoretical predictions and observations of H II regions for Schaerer & de Koter (1997) fluxes compared with those from Kurucz (1991).

The Schaerer & de Koter (1997) fluxes have an additional advantage over Kurucz in that they are coupled to the Geneva stellar evolution code, so that each flux distribution relates to a particular age, luminosity and mass. We shall therefore use the main-sequence (A2–F2) models from Schaerer & de Koter (1997), parameters of which are listed in Table 2. These were calculated with a metallicity of 1/5 Z$_\odot$, appropriate to the metal content of NGC 5253. Two temperature entries provide equivalent O spectral types from these models: Vacca et al. (1996) constructed an empirical $T_{\rm eff}$ calibration based on observational and theoretical results available at the time. An updated OB calibration was provided by Crowther (1997) including more recent results, and omitting the linear $T_{\rm eff}$-spectral type relationship that was assumed by Vacca et al. (1996).

4.4 Extinction effects

We cannot assign a single extinction to the central region of NGC 5253, because the extinction towards the centre is clearly very patchy and irregular [as can be seen in the dust lane and in the Hα/Hβ ratio map of Calzetti et al. (1997)]. Observers have found

Table 2. Stellar parameters and ionizing fluxes of main-sequence O-star flux distributions from Schaerer & de Koter (1997), for 0.2 $Z_\odot$. Approximate spectral types follow the temperature calibrations of Vacca et al. (1996, WDV) and Crowther (1997, PAC).

	Mass $M_\odot$	Age Myr	$T_{\rm eff}$ kK	$\log L_*$ $L_\odot$	$\log Q_{\rm H}$ ph s^{-1}	$\log Q_{\rm He\,I}$ ph s^{-1}	$\log Q_{\rm He\,II}$ ph s^{-1}	Sp. Type WDV	PAC
A2	20	3.6	33.3	4.77	47.84	46.08	0.00	B0 V	O8.5 V
B2	25	2.6	36.3	5.00	48.43	47.42	44.23	O9 V	O8 V
C2	40	1.5	41.7	5.45	49.11	48.53	46.04	O7 V	O6 V
D2	60	0.8	46.1	5.77	49.51	49.02	46.45	O5 V	O4 V
E2	85	0.7	48.5	6.04	49.82	49.36	46.59	O4 V	O3 V
F2	120	0.6	50.3	6.26	50.07	49.62	47.00	O3 V	O3 V

extinction values which range from $A_v \leq 1$ to $A_v = 35$ mag depending on the wavelength, aperture and exact location of the observation. The center of the galaxy is an association of many small regions of greatly differing extinctions; we have here to determine reasonable values of extinction for the hot nucleus and the cooler core.

Calzetti et al. (1997) found that the true nucleus, which we have identified with the [S IV] source, is quite opaque in the visible; comparing the Hα flux with the 2-cm radio they found that the nuclear star cluster is embedded in a cloud of total $A_v = 9$–35 mag. The Brackett α and γ lines of Kawara et al. (1989) give an A_v of 7–12 mag in an area of 10×20 arcsec^2. The extinction to the rest of the core region is much lower, such that the total Hα compared with the 6-cm flux in the inner 38 arcsec gives an A_v of about 1. This agrees with the model that the youngest stars in NGC 5253 are in the nucleus; it is expected that the youngest stars will be the most highly obscured as they have not had time to disperse the dense molecular cloud in which they formed.

For this work we shall use the Kawara et al. (1989) Brγ/Brα ratio since the region sampled by Kawara et al. is comparable to the *ISO* aperture. The relation between the extinction in the IR and A_v is also not well established. Nevertheless, 1 mag of 9.7-μm extinction is estimated to be between 15 and 30 mag of A_v. Although the extinction in the IR is much lower than in the optical, it can still have significant effects on the line ratios. Extinction curves in the IR differ from source to source, but in broad terms the [S IV] and [Ar III] lines will be most affected, and similarly affected, by extinction. From the Kawara et al. Brγ/Brα ratio we find $A_v = 7.7$ mag, $A_K = 0.7$ mag and $A_M = 0.2$ mag using the Howarth (1983) extinction curve. Consequently, the extinction at 9.7 μm is 0.25–0.5 mag, and from the curve of Draine (1989) there is 0.2–0.4 mag of extinction at [Ar III] and [S IV], 0.1–0.2 mag at [S III], 0.08–0.17 mag at [Ne II], and 0.06–0.13 mag at [Ne III].

5 RESULTS OF PHOTOIONIZATION MODELLING

Following the approach described above, we now proceed to determine the massive stellar content in both the starburst nucleus and core of NGC 5253. Fig. 4 shows how selected IR line ratios are affected by changes in temperature and ionization parameter. For a given density, the dependence of line ratios on Q translates into a sensitive function of the input ionization, and thus on the stellar temperature. It is apparent that [S IV] emission is predicted at high Q and $T_{\rm eff}$, while [Ne II] originates from regions of lower Q and $T_{\rm eff}$. [Almost identical contours are obtained using the *solar*-metallicity theoretical flux distributions of Schaerer & de Koter (1997).] We shall now exploit these dependences to derive characteristic stellar temperatures and nebular densities for the two regions under consideration.

5.1 [S IV]-emitting central nucleus

In Section 3 we argued that the [S IV] emission is concentrated in the nuclear region of NGC 5253 observed by Beck et al. (1996). Our principal nuclear diagnostics are therefore: (i) [Ar III]/[S IV] from Beck et al. (1996); (ii) [S IV]/[Ne II] from Beck et al. (1996); (iii) [S IV]/Brα, given that $\sim$30 per cent of the total *ISO* Brα flux is emitted in the nucleus (Section 3.2); (iv) an upper limit on [Ne III]/[S IV] from *ISO*, since [S IV] is formed exclusively in the core; (v) a lower limit on [S IV]/[S III] for similar reasons. [Ne III]/[Ne II] represents a secondary diagnostic since it relies on assumptions regarding the formation of [Ne III] in the nucleus.

In Fig. 4, filled-in circles indicate the position of these IR line ratios in the nucleus. Each diagnostic supports a high ionization parameter for the nucleus. For example, [Ar III]/[S IV] requires solutions in the range ($T_{\rm eff}$/kK, log Q) = (36, 9) to (50, 8) from Fig. 4(f). The observed [S IV]/Brα ratio suggests even higher ionization parameters from Fig. 4(a).

Unfortunately, despite our best efforts, no single solution exists for which all observed line ratios are satisfied. As previous investigators have also found, it is extremely difficult to break the degeneracy between ionization parameter and hardness of the ionizing spectrum from modelling alone. At most two or three are in agreement, suggesting errors in our assumptions relating to line formation regions, photoionization modelling or flux distributions. Table 3 compares selected IR diagnostic ratios at particular temperatures and ionization parameters with observed ratios for the nucleus. We find that optimum agreement is obtained for a narrow 'corridor' ranging in ($T_{\rm eff}$/kK, log Q) from (38, 8.5) to (50, 8.25). Each of these solutions reproduces the observed nebular properties equally well. Consequently, the nucleus is dense and almost certainly contains very early O-type stars. The minimum nuclear stellar temperature corresponds to an O7 V star, and higher temperatures to earlier types. As stated above, the ionization requires 1000 equivalent O7 V stars; if the actual stars are younger, fewer will be needed.

Our principal diagnostic ratios have the basic problem that they combine ions of two different elements and may therefore be in error if the elemental abundances determined by Kobulnicky et al. (1997) are incorrect. This is why ratios of lines from different ions of the same element are usually to be preferred. However, in NGC 5253 the two emission regions appear to be in such extreme states of temperature and ionization parameter that the contribution of one ionic line completely dominates.

5.2 [Ne II]-emitting core

We now discuss constraints on the stellar content and density of the [Ne II]-emitting core region of NGC 5253. Since the [Ar II] line flux

is uncertain (Section 2.2), we are unable to use the [Ar II]/[Ne II] ratio (≤ 0.35) to constrain the core properties. All solutions lie in the range $0.15 \leq$ [Ar II]/[Ne II] ≤ 0.36, assuming a Ne abundance from Kobulnicky et al. (1997) and an Ar abundance of 1/4 solar,

Consequently, our choice of diagnostics for the core region is: (i) [Ne II]/Brα from *ISO*, adjusted for the presence of Brα in the nucleus; (ii) [Ar III]/[Ne II], adjusted for the presence of [Ar III] in the nucleus and the maximum range in line fluxes; (iii) [Si II]34.8 μm/[Ne II], using *ISO* measurements from Genzel et al. (1998), assuming the Si abundance from Kobulnicky et al. (1997) (note that these fluxes were obtained from apertures of different sizes, so this ratio should be treated with caution); (iv) an upper limit on [S III]/[Ne II]. (In reality, [S III] is anticipated to form in both the nucleus and core regions, analogously to [Ar III].) We must wait for mid-IR instruments such as MICHELLE for observational verification of these predictions. The [S IV] flux originating in the core is formally $< 1 \times 10^{-16}$ W m^{-2}, obtained by subtracting the nuclear [S IV] flux of Beck et al. (1996) from the maximum possible *ISO* flux. However, considering sources of uncertainty, a strict upper limit of $< 4 \times 10^{16}$ W m^{-2} is chosen, so that we may additionally use an upper limit on the [S IV]/[Ne II] ratio.

Observed IR line ratios for the core are indicated by open circles in Fig. 4, while Table 3(b) summarizes selected ($T_{\rm eff}$, log Q) combinations. Once again, no single solution exists for which all

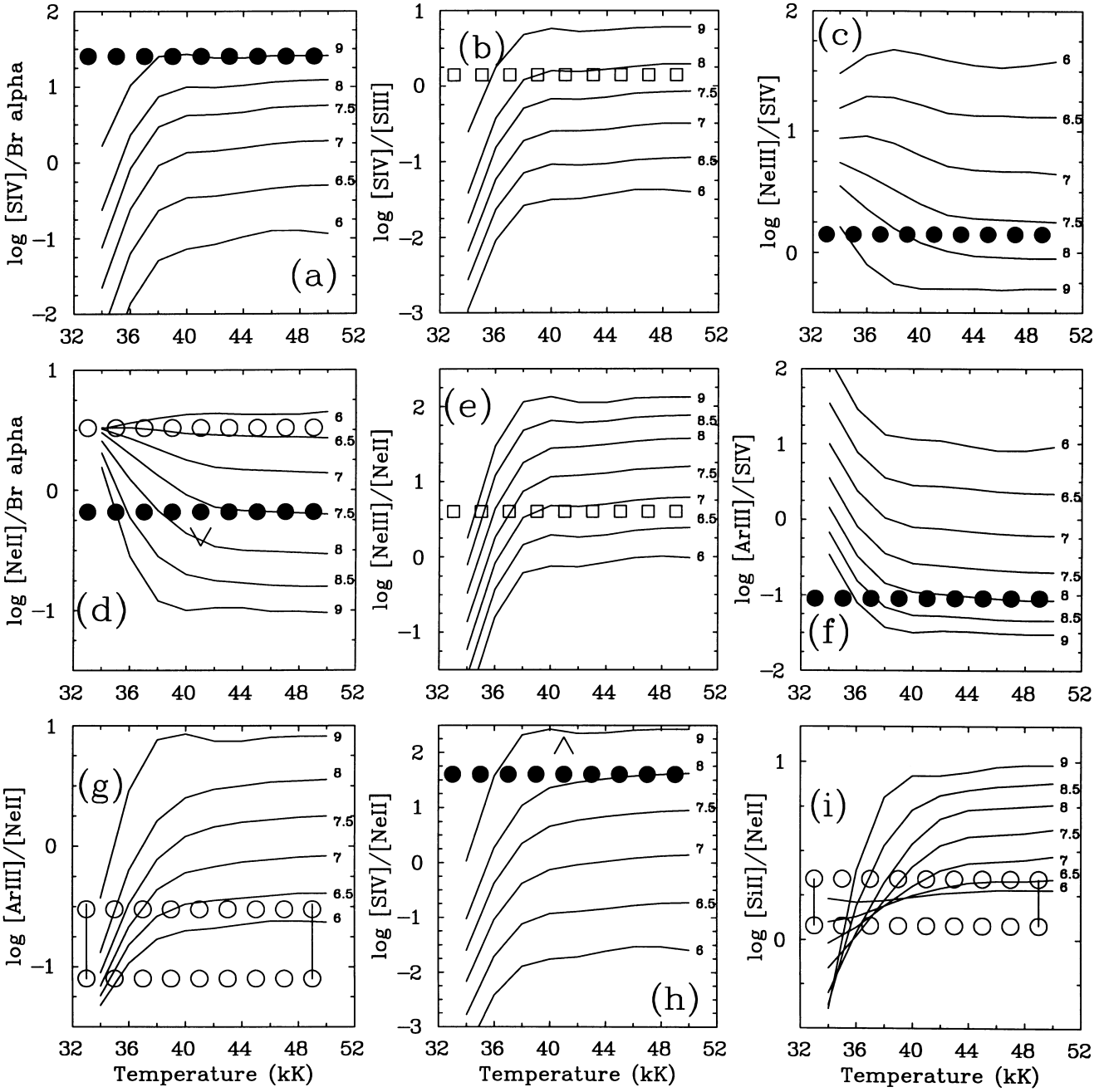

Figure 4. Sensitivity of selected IR line ratios to ionization parameter (Q) and stellar temperature ($T_{\rm eff}$). Circles indicate observed line ratios in the nucleus (filled-in) and core (open), while squares indicate ratios for the combined core–nucleus region. Some observed ratios lie within a particular range of values (connected by solid lines), while others are merely limits (indicated by arrows).

our diagnostics are reproduced. Nevertheless, a very low stellar temperature of 34–36 kK is favoured for the ionizing O stars, with the ionization parameter poorly constrained.

To produce sufficient Lyman continuum ionizing photons for the observed Brα flux in the core requires 2500 equivalent O7 V stars (Section 3.2) – significantly more if the stars are much cooler, as appears to be the case: $T_{\rm eff} \sim 35$ kK corresponds to a stellar type of O8 or O9 (Table 2). Table 3(b) appears to permit ionization parameters as low as $\log Q \sim 6$. However, for this Q-value, the entire volume of the core would only just be sufficient to contain the H II regions associated with 2500 O7 V equivalents. Therefore a higher ionization parameter is favoured, albeit probably lower than for the nucleus of NGC 5253. Stasińska & Leitherer (1996) obtained a fairly tight spread of ionization parameter for young starburst regions.

Combining the above material gives a picture of a hot, dense nucleus with $T_{\rm eff} \geq 38$ kK and $\log Q \sim 8.25$, containing 1000 O7 V equivalents, plus a cooler core of $T_{\rm eff} \sim 35$ kK and $\log Q \leq 8$, with 2 500 O7 V 'equivalents'. It should be noted that the core is cool only by comparison with the nucleus; in a normal star-forming system the low-ionization lines of [Ne II] and [Ar II] dominate the mid-IR spectrum, which is not the case in NGC 5253.

Our results thus far have relied on the validity of the photoionization model CLOUDY. Although this code is widely employed, and has been verified against a suite of other photoionization codes (Ferland et al. 1995), we have performed additional calculations using the shock photoionization code MAPPINGS (Sutherland & Dopita 1993). The MAPPINGS results agree with the overall picture of the hot nucleus in the cooler core, but find rather higher ionization parameters and stellar temperatures for both regions. We believe that this discrepancy can be principally attributed to the use of different O-star flux distributions (Kurucz in the case of MAPPINGS) and may serve as a reminder – and measure – of the disagreements currently

Table 3. (a) Results from photoionization models of individual O stars (Schaerer & de Koter 1997) that are consistent with selected diagnostic IR line ratios for the *nucleus* of NGC 5253. Preferred solutions are indicated by asterisks. (b) As (a), but for the *core* of NGC 5253.

(a)

$T_{\rm eff}$ kK	$\log Q$	[Ar III]/[S IV]	[S IV]/Brα	[Ne III]/[S IV]	[S IV]/[Ne II]	[Ne III]/[Ne II]	[S IV]/[S III]
Observed		0.09	~25	≤1.4	>39	>46?	>1.4
36	9.0	0.08	11	0.8	37	29	1.8
38	8.25	0.10	11	1.1	26	30	1.8
38	8.5	0.07	15	0.9	55	48	2.6*
38	8.75	0.05	20	0.7	115	76	3.5
42	7.75	0.15	7	1.4	13	19	1.0
42	8.25	0.09	15	0.7	56	48	2.5*
42	8.75	0.04	21	0.5	155	83	4.2
46	7.75	0.13	8	1.3	18	22	1.2
46	8.25	0.06	15	0.7	71	50	2.6*
46	8.75	0.04	23	0.5	182	98	4.7
50	7.75	0.13	9	1.2	20	24	1.3
50	8.25	0.06	16	0.7	78	54	2.8*
50	8.75	0.04	23	0.5	190	100	4.8

(b)

$T_{\rm eff}$ kK	$\log Q$	[Ar III]/[Ne II]	[Ne II]/Brα	[Si II]/[Ne II]	[S III]/[Ne II]	[S IV]/[Ne II]
Observed		0.08–0.3	~3.3	1.2–2.2	≤2	<0.35
34	7.25	0.08	3.2	0.8	1.3	0.01
34	8.0	0.13	2.6	0.5	2.3	0.09
34	8.75	0.29	1.8	0.4	3.9	0.62
35	7.0	0.13	3.0	1.0	1.3	0.03
35	7.5	0.17	2.5	0.9	2.1	0.11
35	8.0	0.31	1.7	0.8	3.5	0.47
36	6.0	0.11	3.6	1.6	0.4	0.00
36	6.5	0.15	3.3	1.3	0.8	0.02
36	7.0	0.21	2.7	1.2	1.5	0.09
37	6.25	0.17	3.5	1.5	0.7	0.02

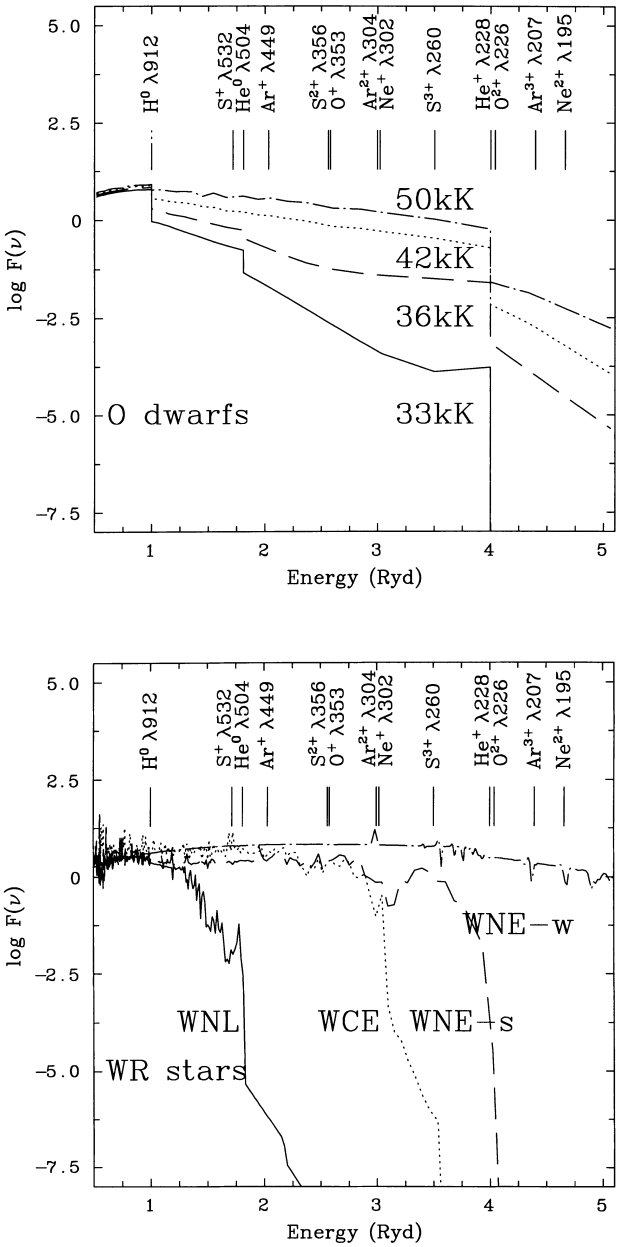

Figure 5. Comparison of the latest Lyman continuum flux distributions from O stars (Schaerer & de Koter 1997) at low metallicity (0.2 $Z_{\odot}$) with recent line-blanketed model atmospheres for WR stars (following Hillier & Miller 1998). It is apparent that strong-lined WCE and WNE stars show similar EUV flux distributions to hot O stars, except that negligible flux is emitted at high energies (3–4 Rydberg), while solely the WNE-w model shows a strong flux above 4 Rydberg ($\lambda \leq 228$ Å). Ionization edges relevant to this study are indicated.

inherent in the use of different photoionization models. To verify our results further we have performed additional calculations, using theoretical WR flux distributions.

6 CONTRIBUTION OF WOLF–RAYET STARS

Up to now we have assumed that O stars are solely responsible for the Lyman ionizing flux from the entire galactic core. However, NGC 5253 is a WR galaxy, with both WN-type and WC-type stars present (Schaerer et al. 1997). Schaerer et al. estimated a population of ≤25 WN stars and 10 WC stars in the nucleus sampled by the ground-based IR data sets of Beck et al. (1996), with an additional 40 WN stars and 13 WC stars located 3 arcsec (60 pc) to the south (also within the *ISO* beam). Schmutz, Leitherer & Gruenwald (1992) have indicated that WR stars produce a harder flux distribution than O-type stars, with significant energy emitted shortward of $\lambda = 228$ Å, except for those stars with the strongest winds. Is it possible that the WR stars of NGC 5253, although few in number, contribute significantly to the high-excitation nebular lines (e.g. [S IV]), and invalidate our earlier conclusions?

6.1 WR flux distributions – what role for line blanketing?

The widely used WR energy distributions of Schmutz et al. (1992) employ non-line-blanketed, pure helium model atmospheres. Models including light metals (e.g. CNO elements) are also in use (e.g. Crowther, Smith & Hillier 1995). Line blanketing by heavy elements (especially Fe) is known to affect the emergent EUV flux distributions dramatically (see e.g. Crowther, Bohannan & Pasquali 1998), but only test model calculations with heavy metals have been published to date (Schmutz 1997; Hillier & Miller 1998), and large grids are not yet available. We have therefore calculated representative line-blanketed models for late WN-type (WNL), strong-lined early WN-type (WNE-s) and early WC-type (WCE) stars at low metallicities ($\sim 0.2\,Z_\odot$) using the Hillier & Miller (1998) approach. We have omitted calculations for late WC stars since they are not considered to exist in low-metallicity environments. The reader is referred to Hillier & Miller (1998) for details of the technique used, except that our calculations include hydrogen, helium, carbon, nitrogen (for WN stars), oxygen (for WC stars) and iron.

Fig. 5 presents a comparison of the EUV flux distributions of these WR models with the Schaerer & de Koter (1997) models of low-metallicity dwarf O stars. WNE-s models incorporating line blanketing show flux distributions in the 228–912 Å range which are fairly similar to the 50-kK O-star model of Schaerer & de Koter (1997) at low metallicity. The strong, line-blanketed WR stellar wind hinders emission below $\lambda = 228$ Å, in contrast with the most recent O-star models. WCE models are similar except that negligible flux is emitted at $\lambda \leq 300$ Å, owing to the blanketing by carbon and oxygen. WNL stars show a much softer energy distribution.

Our results appear in conflict with the much harder fluxes predicted by certain unblanketed models of Schmutz et al. (1992), particularly below the He^+ edge. However, Schmutz et al. correctly stress the importance of stellar wind density, such that emission at $\lambda \leq 228$ Å relies on the WR wind being relatively transparent. Denser winds destroy photons beyond this edge. Does this remain valid for metal-line-blanketed models? In Fig. 5 we include the predicted EUV spectrum for a line-blanketed model of the extremely weak-lined, early-type WN (WNE-w) star HD 104994 (WR46, WN3) using parameters from Crowther et al. (1995), except for a low Fe abundance of $0.2\,Z_\odot$. In agreement with Schmutz et al., the flux distribution for this star is in dramatic contrast with other WR (and O star) line-blanketed models in that it displays a very hard spectrum above the He^+ edge. This is to be expected, since a subset of WR stars do emit a significant flux shortward of $\lambda = 228$ Å, as evidenced from nebular He II λ4686 emission (e.g. Dopita et al. 1990; Garnett et al. 1991).

To test for the influence of WR stars, we have carried out CLOUDY calculations similar to those discussed above. In Table 4,

Table 4. Comparison between IR line ratios predicted in photoionization modelling of NGC 5253 using line-blanketed O-type models (Schaerer & de Koter 1997) and WR distributions (following Hillier & Miller 1998) at $0.2\,Z_\odot$. The O-star $T_{\rm eff}$–spectral type calibration of Crowther (1997) is adopted.

	O dwarfs			Wolf–Rayet stars				
Sp Type	O8.5	O7.5	O6	O3	WNL	WNE-s	WNE-w	WCE
				$\log Q = 8.5$				
Ne III/Ne II	0.4	38.0	60.3	75.9	0.0	69.1	99.9	1.7
S IV/S III	0.1	2.2	3.2	3.8	0.0	4.3	4.9	1.7
Ar III/Ar II	0.5	21.9	24.0	23.4	0.0	28.2	15.2	50.2
Ne II/Brα	2.9	0.3	0.2	0.2	3.3	0.2	0.1	3.0
S IV/Brα	0.4	13.2	17.4	20.0	0.0	23.5	23.0	13.0
O IV/Brα	0.0	0.2	0.2	0.5	0.0	0.0	49.4	0.0
				$\log Q = 7.5$				
Ne III/Ne II	0.1	5.9	12.0	15.8	0.0	15.1	29.8	0.3
S IV/S III	0.0	0.4	0.7	0.8	0.0	1.0	1.7	0.3
Ar III/Ar II	0.2	3.7	9.3	10.2	0.0	12.6	8.9	13.6
Ne II/Brα	3.3	1.5	0.7	0.6	2.7	0.7	0.4	4.1
S IV/Brα	0.0	2.4	4.3	5.6	0.0	7.0	10.8	2.5
O IV/Brα	0.0	0.0	0.0	0.1	0.0	0.0	21.6	0.0
				$\log Q = 6.5$				
Ne III/Ne II	0.0	1.2	1.8	2.5	0.0	2.4	5.5	0.1
S IV/S III	0.0	0.1	0.1	0.1	0.0	0.1	0.3	0.0
Ar III/Ar II	0.1	1.2	2.3	2.6	0.0	3.3	2.8	2.9
Ne II/Brα	3.3	3.2	2.9	2.7	1.4	3.0	2.1	5.0
S IV/Brα	0.0	0.2	0.4	0.5	0.0	0.7	1.5	0.2
O IV/Brα	0.0	0.0	0.0	0.0	0.0	0.0	4.0	0.0

predictions for selected IR line ratios at $\log Q = 6.5$, 7.5 and 8.5 using our WR energy distributions are contrasted with those from a variety of O-star models. These results are now discussed below.

For all realistic ionization parameters, WNL (specifically WN8) stars have negligible contribution to the high-excitation nebular lines observed in the nucleus of NGC 5253, as may be expected from Fig. 5. WNL stars do, however, make contributions to the low-excitation features ([Ne II], [Si II]) in the core of NGC 5253 that are comparable to late O dwarfs. We can safely conclude that the presence of 40–65 WNL stars in NGC 5253 (according to Schaerer et al. 1997) will not significantly affect our earlier results based solely on O stars.

The similarity in the EUV flux distributions of WNE-s and WCE models to early O dwarfs is reflected in their comparable diagnostic line ratios of neon and sulphur. Consequently, the presence of ~23 WC stars in NGC 5253 will not influence our results for either region.

In general, the presence of WR stars in young starburst regions does not affect results from exclusively O stars (however, see below). WNL flux distributions do not differ significantly from those of very late O stars, while WNE-s and WCE energy distributions closely mimic early-type O stars. As we shall see in Section 7, this is in sharp contrast with recent evolutionary synthesis models (Schaerer & Vacca 1998) which utilize the WR models of Schmutz et al. (1992) showing strong emission at $\lambda \leq 228$ Å.

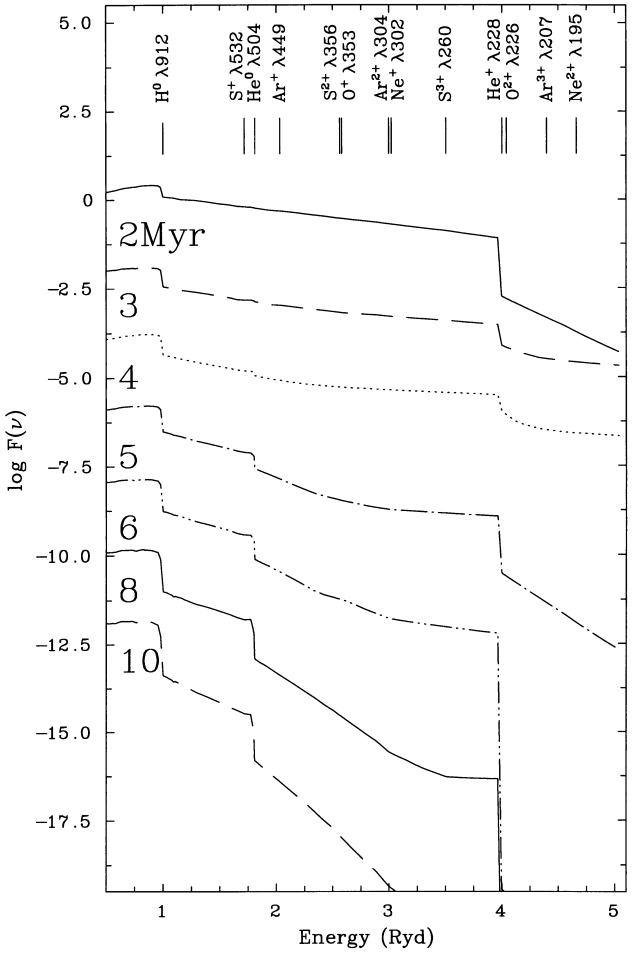

Figure 6. Predictions of flux distributions for a burst of star formation at an age of 2–10 Myr from Schaerer & Vacca (1998) at $Z = 0.2\ Z_{\odot}$, using the Meynet et al. (1994) evolutionary tracks coupled with O-star flux distributions from Schaerer & de Koter (1997), plus Schmutz et al. (1992) WR models, present between 2.8 and 5.2 Myr (causing the hard EUV flux distribution). Ionization edges are indicated.

6.2 WR stars as the source of [O IV] emission in starbursts?

Lutz et al. (1998) have recently proposed the identification of [O IV]25.91-μm emission in several young starburst galaxies, including NGC 5253. They suggest that WR stars may provide the hard ionizing flux necessary for such a highly excited feature. Our *ISO* spectrum suggests an upper limit for the [O IV] line of 0.1×10^{-16} W m^{-2} or [O IV]/Brα ≤ 0.07, reasonably assuming that any emission is restricted to the nuclear region. (Lutz et al. report 0.65×10^{-16} W m^{-2} based on data sets of higher signal-to-noise ratio, implying [O IV]/Brα~0.35.) Our observations indicate that [Ne V]14.3 μm is not present in NGC 5253.

Line blanketing softens the flux from the majority of early-type WR stars, such that negligible nebular [O IV]25.9-μm emission is predicted from photoionization models of such stars, in contrast with early O stars (Table 4). This is the precise opposite of predictions using earlier O and WR models (Kurucz 1991; Schmutz et al. 1992)! Within the high ionization parameter nucleus of NGC 5253, the low-metallicity grids of Schaerer & de Koter (1997) predict that observable nebular [O IV] could be produced by early O dwarfs: [O IV]/Brα ~ 0.5 for O3 V stars at $\log Q \sim 8.5$.

However, certain WR stars emit large numbers of photons with energies above the He II λ228 edge, necessary for [O IV] emission. We include results of photoionization modelling of the WNE-w flux distribution in Table 4. From the table, [O IV]25.9-μm emission is predicted at all ionization parameters, two orders of magnitude greater than O3 V stars at parameters appropriate for the nucleus of NGC 5253! Other high-ionization IR nebular lines are predicted, including [Ne V]14.3 μm ([Ne V]/Brα ~ 6 at $\log Q = 8.5$).

Since such emission features are not prominent in our *ISO* observations, we can exclude the possibility of a significant number of such stars being present in NGC 5253. This is expected, since WNE-w stars are very rare in our Galaxy and the Magellanic Clouds. They have unusually low-emission line fluxes.[1] Consequently, their identification would prove difficult in external galaxies from optical spectroscopic techniques.

Our results suggest that WR stars will only play a major role in the overall energy distribution of a young starburst region if they are very hot, and possess stellar winds that are relatively transparent. In the nearby Universe such stars are rare, so it is unlikely that they represent the 'Warmers' responsible for the high IR excitation features observed in active galactic nuclei (Terlevich & Melnick 1985). However, metallicity also complicates matters yet further, affecting both the degree of EUV line blanketing and the strength of the stellar wind (although a metallicity dependence of mass loss in WR stars has yet to be established observationally). If such a dependence were identified, weaker stellar winds *would* yield harder EUV flux distributions. Such a result would have an important effect on the possibility of WR stars providing the hard ionizing flux in very metal-poor starbursts, such as I Zw 18 (de Mello et al. 1998). More definitive answers await the calculation of a grid of line-blanketed WR models for various combinations of mass-loss rates and metallicity. Crowther (1999) discusses this aspect in greater detail.

[1] WR 46 has a He II λ4686 emission-line flux of 1.2×10^{35} erg s^{-1}, which is a factor of 4 lower than typical WNE stars (Schaerer & Vacca 1998).

7 PHOTOIONIZATION PREDICTIONS FOR A BURST OF STAR FORMATION

Our photoionization modelling has used a single O- or WR-star flux distribution, adjusted to differing ionization parameters. In reality, the nucleus and core of NGC 5253 will contain stars spanning an enormous range of masses and temperatures, even if they were formed in a single burst of star formation. So, how valid is our assumption that the most massive (and consequently the highest temperature) stars dominate the IR nebular line fluxes? To investigate this, we have kindly been provided with evolutionary synthesis models (v2.32) from Schaerer & Vacca (1998). These utilize the low-metallicity ($0.2\,Z_{\odot}$) Schaerer & de Koter (1997) flux distributions for O-type stars, a Salpeter IMF and a mass range of $0.8-120\,M_{\odot}$ and were calculated for differing ages according to the Meynet et al. (1994) evolutionary tracks after an instant burst of star formation.

Fig. 6 presents EUV flux distributions produced by these models for different ages. Excess high-energy photons at $\lambda \leq 228$ Å are produced by WN and WC stars between 2.8 and 5.2 Myr, since Schaerer & Vacca (1998) utilized the low wind density Schmutz et al. (1992) WR model distributions. From Section 6 such EUV excesses may be in error. Nevertheless, detailed comparisons may be made with our predictions based on single O-star models,

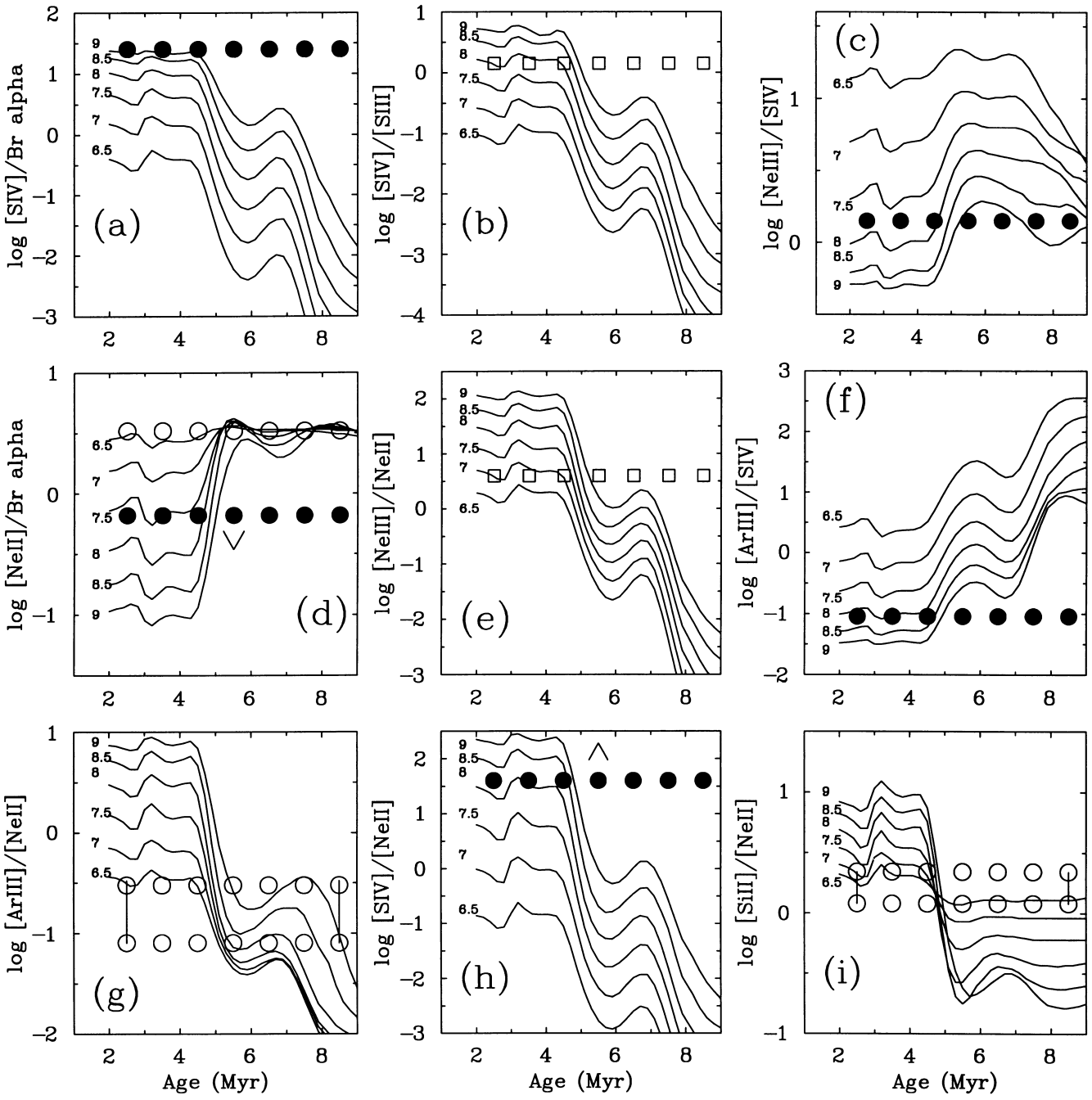

Figure 7. Sensitivity of selected IR line ratios to ionization parameter (Q) and age (Myr) for the instantaneous burst models from Schaerer & Vacca (1998) at $Z = 0.2\,Z_{\odot}$. Symbols are as in Fig. 4.

treating specific results during the WR phase with caution. We have generated a grid of photoionization models for ages in the range 2–10 Myr, and calculated fluxes for a fixed density of 10 cm^{-3}, with a total luminosity of 10^1, 10^2, ..., 10^{11} $L_\odot$, which covers a range in ionization parameter similar to our earlier calculations. The sensitivity of IR diagnostic line ratios to ionization parameter and age (in Myr) is presented in Fig. 7, where we again include observed line ratios in the nucleus (filled circles), core (open circles) and combined core–nucleus region (open squares).

In Table 5(a) we present selected age and ionization parameter solutions that are in reasonable agreement with our IR diagnostics in the nucleus. The degree of consistency between alternative diagnostics is comparable to those from individual O-star flux distributions (Table 3a). Our earlier results for the nuclear region ionization parameter are supported, with $\log Q \sim 8$–8.5. The precise age is difficult to constrain tightly, but ages in the range 2–4 Myr are in reasonable agreement with the observed line ratios. Recalling that the synthesis calculations between 2.9 and 4.7 Myr are strongly affected by the presence of hot WR stars, our preferred solution is 2–3 Myr.

Table 5. (a) Results from photoionization models of evolutionary synthesis calculations for an instantaneous burst at 0.2 $Z_\odot$ (Schaerer & Vacca 1998) that are consistent with selected diagnostic IR line ratios for the *nucleus* of NGC 5253. Our preferred solutions (indicated by asterisks) are prior to the hot WR phase (2.9–4.7 Myr) because of the uncertain WR flux distributions assumed in the models. (b) As (a), but for the *core* of NGC 5253.

(a)

Age Myr	log Q	[Ar III]/[S IV]	[S IV]/Brα	[Ne III]/[S IV]	[S IV]/[Ne II]	[Ne III]/[Ne II]	[S IV]/[S III]
Observed		0.09	~25	≤1.4	>39	>46?	>1.4
2.0	8.0	0.10	10	1.0	14	30	1.7
2.0	8.25	0.07	14	0.7	60	45	2.4*
2.0	8.5	0.08	18	0.6	102	63	3.3
2.5	8.0	0.11	9	1.1	21	24	1.3
2.5	8.25	0.08	12	0.8	43	35	2.0*
2.5	8.5	0.06	16	0.7	79	52	2.8
3.0	8.0	0.09	10	1.0	34	32	1.7
3.0	8.25	0.07	14	0.7	66	48	2.5*
3.0	8.5	0.05	18	0.6	117	71	3.5
4.0	8.0	0.10	10	1.0	30	30	1.6
4.0	8.25	0.07	13	0.8	59	45	2.3
4.0	8.5	0.05	16	0.6	100	63	3.0
4.5	8.25	0.09	10	0.9	35	32	1.7
4.5	8.5	0.08	11	0.8	68	33	2.0
4.5	8.75	0.05	17	0.6	112	68	3.4

(b)

Age Myr	log Q	[Ar III]/[Ne II]	[Ne II]/Brα	[Si II]/[Ne II]	[S III]/[Ne II]	[S IV]/[Ne II]
Observed		0.08–0.3	~3.3	1.2–2.2	≤2	<0.35
4.6	6.25	0.18	3.5	1.6	1.0	0.02
4.7	6.0	0.12	4.2	1.7	0.4	0.01
4.7	6.5	0.18	3.2	1.5	0.9	0.03
4.7	7.0	0.29	2.4	1.4	1.9	0.19
5.0	6.75	0.10	3.3	1.1	0.9	0.02
5.0	7.5	0.14	2.9	0.7	1.8	0.13
5.0	8.25	0.27	2.1	0.4	3.1	0.83
5.2	7.5	0.08	3.6	0.5	1.3	0.05
5.2	8.0	0.11	3.7	0.3	1.7	0.15
5.2	8.5	0.19	2.7	0.2	2.4	0.55

For the core, Table 5(b) presents results of our photoionization models that are in reasonable agreement with our chosen mid-IR diagnostics, although the level of agreement is no better than that obtained from individual O-star flux distributions (Table 3b). Once again, we find that the core ionization parameter remains uncertain, with $\log Q = 6.5$ to 8 providing reasonable agreement for a fairly narrow range of ages, between 4.7 and 5.2 Myr. The only WR stars predicted during this age range are late WN stars, with a fairly soft EUV distribution, so that the evolutionary synthesis models should be appropriate. A significantly older population (5–10 Myr) would require a very low ionization parameter ($\log Q \sim 6$). As previously indicated, the entire volume of the core would only just be sufficient to contain the H II regions associated with 2500 O7 V equivalents for this Q-value, so we can exclude such a population.

Overall, our results from earlier calculations are broadly supported here, based on more sophisticated flux distributions. Consequently, an important result from this work is that meaningful results may be obtained for very young starburst regions based on individual O-star flux distributions alone.

8 COMPARISON WITH PREVIOUS DETERMINATIONS

We now compare our present results for the hot, massive stellar content in NGC 5253 with those obtained previously from ground- (Aitken et al. 1982; Beck et al. 1996) and space-based (Lutz et al. 1996) IR observations, as summarized in Table 6. (We are unaware of any studies based on optical data sets.)

All previous mid-IR analyses relied on: (i) O-star flux distributions that did not account for non-LTE effects or stellar winds, or in many cases the low metallicity of the galaxy; (ii) inappropriate line ratios (given the results from ground- and space-based observations); and (iii) assumed elemental abundances (often solar composition) and ionization parameter. Consequently, previous approaches may lead to imprecise results, although all studies support the presence of hot, young O-type stars in the central starburst, with characteristic temperatures ranging from 40 to ≥50 kK.

Our comparison with previous results well illustrates the effect of different O-star flux distributions and elemental abundances, even with an identical photoionization code and IR line diagnostics being employed. For example, Lutz et al. (1996) obtained a characteristic O-star temperature of 48.5 kK from the observed [Ne III]/[Ne II] ratio, since they adopted *solar* Kurucz (1991) models, *solar* elemental abundances and $\log Q = 8$. From our analysis, neglecting the spatial information for line formation in NGC 5253 and adopting $\log Q = 8$ imply a stellar temperature of 36 kK for the combined core–nucleus region using [Ne III]/[Ne II] from Fig. 4(e). Alternatively, a stellar temperature of 39 kK would result from the observed [S IV]/[S III] ratio with an identical ionization parameter (Fig 4b).

Having established constraints on the stellar content of the nucleus and core of NGC 5253, we are able to compare ages obtained from the derived stellar temperatures with those from evolutionary synthesis calculations. A minimum characteristic stellar temperature of ≥38 kK for the nucleus implies a minimum characteristic mass of ~35 $M_\odot$. Using the result of Kunze et al. (1996) that the upper mass cut-off of a cluster is about 5 $M_\odot$ greater than the single-star equivalent mass gives a lower limit to the mass cut-off of 40 $M_\odot$ for the hot nucleus, with an age no greater than around 3 Myr (Meynet et al. 1994). This is in reasonable agreement

Table 6. Summary of comparison between stellar temperatures and ionization parameters derived for NGC 5253 using IR diagnostics. Theoretical O-star fluxes are from Hummer & Mihalas (1970, HM70), Kurucz (1991, K91) and Schaerer & de Koter (1997, SdK97), while photoionization models employed are MAPPINGS II (Sutherland & Dopita 1993, SD93) and CLOUDY (Ferland 1996, F96).

Study	IR diagnostics	– O star Fluxes – Ref.	$Z_\odot$	Photo-Code	Abund. $Z_\odot$	$T_{\rm eff}$ kK	log Q	Age Myr	Notes
Aitken et al. 1982	[S IV]	HM70	1.0	–	1.0	≥50	–		
Beck et al. 1996	[S IV], [Ar III], [Ne II]	K91	0.1–1.0	SD93	1.0	40–45	–	–	
Lutz et al. 1996	[Ne II–III]	K91	1.0	F96	1.0	48.5	8.0	–	Q assumed
This work (nucleus)	[S IV], [Ar III], [Ne III], Brα	SdK97	0.2	F96	0.25	38–50	~8.25	2–3	
This work (core)	[Ne II], [Ar III], [S III], Brα	SdK97	0.2	F96	0.25	~35	≤8	4.7–5.2	

with the evolutionary synthesis calculations for $\log Q \sim 8$, and is typical of recent age estimates for the central nucleus of NGC 5253 from the WR population (Schaerer et al. 1997). [For $T_{\rm eff} \approx 46$ kK the implied hottest stellar type is O4 or O5 with mass $\sim 60\,M_\odot$ at a corresponding age of ~2.5 Myr.]

For the core region, a stellar temperature of ~35 kK corresponds to the hottest spectral type being equal to or later than O8 V or O9 V (Table 2), and an equivalent mass of $\sim 25\,M_\odot$. This gives an upper mass cut-off of $30\,M_\odot$, indicating an age of around 4–5 Myr, in good agreement with that implied from our synthesis calculations. However, we note that our determination is based on the entire core of NGC 5253, spanning several hundred parsecs. We do not claim that the massive stellar population in the core of NGC 5253 was formed coevally ~5 Myr ago. Our results are almost certainly biased towards the youngest, most massive clusters exterior to the central nucleus. In reality, the content of the core will span a large range of ages. The weakness of [Ar II] emission does appear to rule out a particularly old population. Vanzi & Rieke (1997) concluded from near-IR spectroscopy that NGC 5253 is young (~8 Myr) and contains high-temperature stars (≥40 kK), since He I 1.70 μm is present, and [Fe II] emission (from supernova remnants) is very weak, as are the CO absorption bands (produced by red giants). Davies et al. (1998) estimated a greater age of ~10–12 Myr for regions ~7 arcsec from the central nucleus.

Again, neglecting the spatial origin of low- and high-excitation lines and assuming a uniform ionization parameter of $\log Q = 8$, an age of ~4.8 Myr is obtained from [Ne III]/[Ne II] following Fig. 7(e). Alternatively, an age of either 2.9 or 4.4 Myr is implied from the observed [S IV]/[S III] ratio (Fig. 7b).

To summarize, many models and techniques may be applied to IR observations of this galaxy. While they differ in details, they agree with each another in the general picture of NGC 5253. This galaxy has a very young starburst in the nucleus and a slightly older one within the core. It is remarkable for the youth of the starburst, probably no more than 3 Myr old, and for the very massive stars that it formed. [For stars to reach the WC phase in such a low-metallicity environment requires very massive progenitors of $60–120\,M_\odot$ (Maeder & Meynet 1994).]

9 DISCUSSION AND CONCLUSIONS

NGC 5253 is widely acknowledged to be an excellent, in some respects unequalled, laboratory for the study of intense starbursts. This is because it is relatively close and contains a very young starburst, and because its central region is so varied, containing many sub-regions and clusters of different ages and stellar content. (The patchiness of the central region of NGC 5253 is probably related to its extreme youth: there has not been time for stars to migrate away from their points of formation and for the original structure of star formation to be lost.) NGC 5253 also has the special advantage of dwarf galaxies: in contrast with large spiral galaxies, bursts are seen against a very low interburst star formation rate rather than steady star formation activity.

It is therefore rather troubling that the properties of NGC 5253 at which we arrive in this paper depend so crucially on the high spatial resolution ground-based data. The characteristics of NGC 5253 that make it so interesting also make it very hard to interpret observations that could not, for example, distinguish between the nucleus and core. If we had not been able to assign the different infrared lines to their appropriate sources, we would have found highly contradictory line ratios and an imprecise effective stellar temperature of the ionizing O stars. Even with the existing ground- and space-based observations, some important results await confirmation: e.g. what fraction of the [S III] nebular flux is located in the nucleus?

Nevertheless, it is clear from our results that the nucleus of NGC 5253 contains extremely young, massive, hot stars, with a high characteristic ionization parameter. The surrounding core contains cooler stars, with a lower ionization parameter, and undoubtedly contains stars spanning a wide range of ages. The nucleus of NGC 5253 is not unique in this respect: the stellar content of 30 Doradus in the Large Magellanic Cloud, for example, shares many of its attributes, and deserves greater study at mid-IR wavelengths. One important result of our study is that estimating the global properties of young starbursts from the effective temperatures of their most massive constituents appears to be a reasonable approach.

Unfortunately, it is not yet possible readily to compare the spatial density of O stars in the super-star nucleus of NGC 5253 with that of other giant H II regions. Definitive answers await high spatial resolution IR observations, but the ionization parameter for the nucleus indicates a dense concentration. At the very least, 1000 O7 V 'equivalents' occupy a region of radius ≤15 pc. For comparison, ~100 early O stars, with a *similar* total Lyman ionizing flux, are located within a radius of 10 pc from R136a in 30 Doradus (Massey & Hunter 1998; Crowther & Dessart 1998).

Our principal result illustrates the challenge faced by nearly all observations of galaxies: many different sources fall into a single aperture. This is particularly acute for dwarf starburst galaxies, where there is less background of star formation, where the smoothing effects of shear and spiral arm forces are absent, and where the starburst activity is likely to be concentrated in one or a few clumps a few parsecs in size. Consequently, high spatial resolution observations of NGC 5253 and other nearby starbursts are urgently sought at near-IR and mid-IR wavelengths, and quantitative results for distant starbursts should, for the moment, be treated with caution.

ACKNOWLEDGMENTS

This work is based on observations with *ISO*, an ESA project with instruments funded by ESA Member States (especially the PI countries: France, Germany, the Netherlands and the United Kingdom) with the participation of ISAS and NASA. We thank John Hillier for providing his stellar atmosphere code and Daniel Schaerer for providing us with his grid of evolutionary synthesis calculations, and appreciate useful discussions with Gary Ferland and Jean-René Roy. An anonymous referee provided extremely useful comments on this work. PAC is a Royal Society University Research Fellow. SCB was supported by the US–Israel Binational Science Foundation grant 94-00303. PSC appreciates hospitality at University College London where the initial proposal for this work was first begun. This research has made use of the NADA/IPAC Extragalactic Database (NED), which is operated by the Jet Propulsion Laboratory, California Institute of Technology, under contract with the National Aeronautics and Space Administration.

REFERENCES

Aitken D. K., Roche P. K., Allen M. C., Phillips M. M., 1982, MNRAS, 199, 31P
Baldwin J. A., Ferland G. J., Martin P. G., Corbin M. R., Cota S. A., Peterson B. M., Slettebak A., 1991, ApJ, 374, 580
Beck S. C., Turner J. L., Ho P. T. P., Lacy J. H., Kelly D. M., 1996, ApJ, 457, 610
Calzetti D., Meurer G. R., Bohlin R. C., Garnett D. R., Kinney A. L., Leitherer C., Storchi-Bergman T., 1997, AJ, 114, 1834
Crowther P. A., 1997, in Bedding T. R., Booth A. J., Davis J., eds, Proc. IAU Symp. 189, Fundamental Stellar Properties: The Interaction between Observation and Theory. Kluwer, Dordrecht, p. 137
Crowther P. A., 1999, in van der Hucht K. A., Koenigsberger G., Eenens P. R. J., eds, Proc. IAU Symp. 193, Wolf–Rayet Phenomena in Massive Stars and Starburst Galaxies, in press
Crowther P. A., Dessart L., 1998, MNRAS, 296, 622
Crowther P. A., Smith L. J., Hillier D. J., 1995, A&A, 302, 457
Crowther P. A., Bohannan B., Pasquali A., 1998, in Howarth I. D., ed., ASP Conf. Ser. Vol. 131, Boulder–Munich II: Properties of Hot, Luminous Stars. Astron. Soc. Pac., San Francisco, p. 38
Davies R. I., Sugai H., Ward M. J., 1998, MNRAS, 295, 43
de Graauw Th. et al., 1996, A&A, 315, L49
de Mello D. F., Schaerer D., Heldman J., Leitherer C., 1998, ApJ, 507, 199
de Vaucouleurs G., de Vaucouleurs A., Corwin H. G., Jr, Buta R. J., Paturel G., Fouqué P., 1993, Third Reference Catalogue of Bright Galaxies. Springer-Verlag, New York
Dopita M. A., Lozinskaya T. A., McGregor P. J., Rawlings S. J., 1990, ApJ, 351, 563
Draine B. T., 1989, in Kaldeich B. H., ed., Infrared Spectroscopy in Astronomy. ESA, Paris, p. 93
Ferland G. J., 1996, HAZY, a Brief Introduction to CLOUDY 90, University of Kentucky, Physics Department Internal Report (F96)
Ferland G. J. et al., 1995, in Williams R. E., Livio M., eds, Analysis of Emission Lines, A meeting Honoring the 70th Birthdays of D. E. Osterbrock and M. J. Seaton. Cambridge Univ. Press, Cambridge
Ferland G. J., Korista K. T., Verner D. A., Ferguson J. W., Kingdon J. B., Verner E. M., 1998, PASP, 110, 761
Garnett D. R., Kennicutt R. C., Chu Y-. H., Skillman E. D., 1991, PASP, 103, 850
Genzel R. et al., 1998, ApJ, 498, 579
Gorjian V., 1996, AJ, 112, 1886
Hillier D. J., Miller D. L., 1998, ApJ, 496, 407
Howarth I. D., 1983, MNRAS, 203, 301
Howarth I. D., Murray J., Mills D., Berry D. S., 1995, Starlink User Note 50.16, Rutherford Appleton Laboratory
Hummer D. G., Mihalas D., 1970, MNRAS, 147, 339 (HM70)
Kawara K., Nishida M., Phillips M. M., 1989, ApJ, 337, 230
Kennicutt R. C., 1984, ApJ, 287, 116
Kessler M. et al., 1996, A&A, 315, L27
Kobulnicky H. A., Skillman E. D., Roy J. R., Walsh J. R., Rosa M. R., 1997, ApJ, 477, 679
Kunze D. et al., 1996, A&A, 315, L101
Kurucz R. L., 1991, in Philip A. G. D., Upgren A. R., Janes K., A., eds, Precision Photometry: Astrophysics of the Galaxy. L. Davis Press, Schenectady, p. 27 (K91)
Lutz D. et al., 1996, A&A, 315, L137
Lutz D., Kunze D., Spoon H. W. W., Thornley M. D., 1998, A&A, 333, L75
Maeder A., Meynet G., 1994, A&A, 287, 803
Martin C. L., Kennicutt R. C., 1995, ApJ 447, 171
Massey P., Hunter D. A., 1998, ApJ, 493, 180
Meynet G., Maeder A., Schaller G., Schaerer D., Charbonnel C., 1994, A&AS, 103, 97
Saha A., Sandage A., Labhardt L., Schwengler H., Tammann G. A., Panagia N., Macchetto D. F., 1995, ApJ, 438, 8
Schaeidt S. et al., 1996, A&A, 315, L60
Schaerer D., de Koter A., 1997, A&A, 322, 615 (SdK97)
Schaerer D., Vacca W. D., 1998, ApJ, 497, 618
Schaerer D., Contini T., Kunth D., Meynet G., 1997, ApJ, 481, 75
Schmutz W., 1997, A&A, 321, 268
Schmutz W., Leitherer C., Gruenwald R., 1992, PASP, 104, 1164
Sellmaier F., Yamamoto T., Pauldrach A. W. A., Rubin H., 1996, A&A, 305, L37
Stasińska G., Leitherer C., 1996, ApJS, 107, 661
Stasińska G., Schaerer D., 1997, A&A, 322, 615
Stevens I. R., Strickland D. K., 1998, MNRAS, 294, 523
Storey P. J., Hummer D. G., 1995, MNRAS, 272, 41
Sutherland R. S., Dopita M. A., 1993, ApJS, 88, 253 (SD93)
Terlevich R., Melnick J., 1985, MNRAS, 213, 841
Turner J. L., Beck S. C., Hurt R. L., 1997, ApJ, 474, L11
Turner J. L., Ho P. T. P., Beck S. C., 1998, ApJ, 116, 1212
Vacca W.D, 1994, ApJ, 421, 140
Vacca W. D., Conti P. S., 1992, ApJ, 401, 543
Vacca W. D., Garmany C. D., Shull J. M., 1996, ApJ, 460, 914
Valentijn E. A. et al., 1996, A&A, 315, L60
Vanzi L., Rieke G. H., 1997, ApJ, 479, 794
Walsh J. R., Roy J.-R., 1989, MNRAS, 239, 297

This paper has been typeset from a T_EX/L^AT_EX file prepared by the author.